Werk

Jahr: 1979
Kollektion: fid.geo
Signatur: 8 Z NAT 2148:46
Digitalisiert: Niedersächsische Staats- und Universitätsbibliothek Göttingen
Werk Id: PPN1015067948_0046
PURL: http://resolver.sub.uni-goettingen.de/purl?PPN1015067948_0046

LOG Id: LOG_0023
LOG Titel: The geomagnetic field ans its secular variation on Finland and Nearby Countries
LOG Typ: article

Übergeordnetes Werk

Werk Id: PPN1015067948
PURL: http://resolver.sub.uni-goettingen.de/purl?PPN1015067948
OPAC: http://opac.sub.uni-goettingen.de/DB=1/PPN?PPN=1015067948

Contact

Niedersächsische Staats- und Universitätsbibliothek Göttingen
Georg-August-Universität Göttingen
Platz der Göttinger Sieben 1
37073 Göttingen
Germany
Email: gdz@sub.uni-goettingen.de

J. Geophys. 46, 201–216, 1979

Journal of Geophysics

The Geomagnetic Field and Its Secular Variation in Finland and Nearby Countries

H. Nevanlinna*

Department of Geophysics, University of Helsinki, Vironkatu 7B, SF-00170 Helsinki 17, Finland

Abstract. All magnetic observations made in Finland before 1910 and certain field measurements and observatory results up to 1970 were used to calculate polynomials representing the geomagnetic field in Finland before 1970. Fourth degree polynomials in time and first degree in latitude and longitude were found to fit the observations with r.m.s. errors of 235nT in H, 0.9° in D and 0.3° in I.

Equivalent dipoles for the magnetic field and its secular variation since 1840 were calculated. By comparing these dipoles with global data, it was found that the nondipole field has been increasing in Finland and nearby countries, and that the secular variation is closely connected with changes in the large nondipole anomaly in Central Asia and with the global 60-year oscillation of the Earth's magnetic field.

Key words: Geomagnetic field – Secular variation – Polynomials – Finland – Equivalent dipoles.

Introduction

Between 1650 and 1910 some 350 measurements of the declination (D), inclination (I) and horizontal intensity (H) of the geomagnetic field had been made in Finland (Nevanlinna and Sucksdorff, 1976). These measurements had only been made sporadically and there had been no long-term recordings to determine the secular variation. Thanks to the growing number of systematic geomagnetic recordings and large-scale surveys, the geomagnetic field and its secular variation in Finland has been well known since 1910.

The main purpose of this paper is to visualize the large-scale geomagnetic field and its secular variation, especially before 1910, by means of graphs and polynomials. Sources of the geomagnetic field in Finland and nearby countries have been analyzed using simple dipole models.

* Department of Geophysics, University of Helsinki, and Finnish Meteorological Institute, Helsinki

0340-062X/79/0046/0201/$03.20

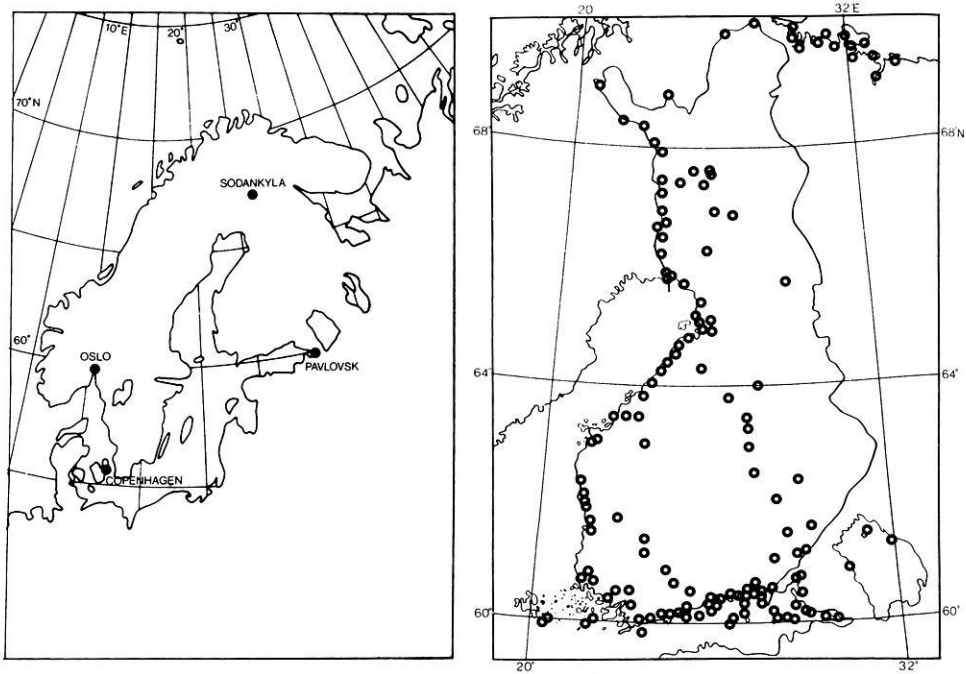

Fig. 1. *Left:* The geomagnetic observatories shown in Figs. 2–4. *Right:* Sites of geomagnetic measurements made before 1910

1. The Geomagnetic Field Expressed by Polynomials

Polynomials are widely used to depict evenly distributed and smoothly varying geomagnetic fields in limited areas like Finland. They enable any component C of the geomagnetic field to be expressed as a function of latitude ϕ, longitude λ and time t, as follows:

$$C(\phi, \lambda, t) = m_0(t) + m_1(t)(\phi - \phi_c) + m_2(t)(\lambda - \lambda_c) + m_3(t)(\phi - \phi_c)^2 + \ldots \quad (1a)$$

where the coefficients $m_i(t)$ are also polynomials:

$$m_i(t) = n_{i0} + n_{i1}(t - t_c) + n_{i2}(t - t_c)^2 + \ldots \quad (1b)$$

where the coefficients n_{ij} are constants and ϕ_c, λ_c, and t_c are fixed points generally near the middle point of the observations.

The only geomagnetic observations available for Finland before 1910 are 350 observations of H, D, and I, made sporadically at different sites and epochs. Figure 1 shows the sites of all these measurements; a full list of them has been published by Nevanlinna and Sucksdorff (1976). The polynomial selected to represent the H, D, and I components of these measurements, based on Eqs. (1a)

Table 1. The coefficients n_{ij} and their standard deviations σ_{ij} of the H, D, and I polynomials in Eq. (2). D and I are given in arcdegrees and H in nanoteslas (nT)

ij	H		D		I	
	n_{ij}	σ_{ij}	n_{ij}	σ_{ij}	n_{ij}	σ_{ij}
00	$0.14522 \cdot 10^5$	$0.15 \cdot 10^3$	-7.59	0.10	$0.7288 \cdot 10^2$	0.15
01	$0.16996 \cdot 10^2$	5.10	$0.967 \cdot 10^{-1}$	$0.34 \cdot 10^{-2}$	$-0.2327 \cdot 10^{-1}$	$0.71 \cdot 10^{-2}$
02	0.30336	0.16	$0.729 \cdot 10^{-3}$	$0.34 \cdot 10^{-4}$	$0.5619 \cdot 10^{-4}$	$0.18 \cdot 10^{-3}$
03	$-0.13086 \cdot 10^{-1}$	$0.29 \cdot 10^{-2}$	$-0.443 \cdot 10^{-5}$	$0.50 \cdot 10^{-6}$	$0.8771 \cdot 10^{-5}$	$0.24 \cdot 10^{-5}$
04	$0.75483 \cdot 10^{-4}$	$0.15 \cdot 10^{-4}$	$-0.249 \cdot 10^{-7}$	$0.26 \cdot 10^{-8}$	$-0.5685 \cdot 10^{-7}$	$0.12 \cdot 10^{-7}$
10	$-0.33973 \cdot 10^3$	$0.30 \cdot 10^2$	$0.386 \cdot 10^{-1}$	$0.23 \cdot 10^{-1}$	0.5272	$0.39 \cdot 10^{-1}$
11	-1.3979	1.11	$-0.114 \cdot 10^{-2}$	$0.37 \cdot 10^{-3}$	$0.1452 \cdot 10^{-2}$	$0.14 \cdot 10^{-2}$
12	$0.79346 \cdot 10^{-2}$	$0.92 \cdot 10^{-3}$	$0.282 \cdot 10^{-4}$	$0.64 \cdot 10^{-5}$	$-0.1290 \cdot 10^{-4}$	$0.12 \cdot 10^{-4}$
20	$0.49864 \cdot 10^2$	$0.35 \cdot 10^2$	0.643	$0.21 \cdot 10^{-1}$	$-0.3854 \cdot 10^{-2}$	$0.44 \cdot 10^{-1}$
21	$0.55469 \cdot 10^{-1}$	$0.14 \cdot 10^{-1}$	$-0.938 \cdot 10^{-3}$	$0.66 \cdot 10^{-3}$	$-0.1659 \cdot 10^{-3}$	$0.15 \cdot 10^{-2}$
22	$-0.55672 \cdot 10^{-2}$	$0.11 \cdot 10^{-1}$	$0.169 \cdot 10^{-4}$	$0.97 \cdot 10^{-5}$	$0.5494 \cdot 10^{-5}$	$0.55 \cdot 10^{-4}$

Table 2. R.m.s. differencies between polynomial and observed values of H, D, I, and Z. (Numbers of observations in brackets)

Year	-1800	$1800-25$	$1825-50$	$1850-75$	$1875-00$	$1900-25$	$1925-$	Total
H			245 (62)	230 (33)	415 (75)	165 (44)	135 (196)	$235\,nT$ (410)
D	2.7 (18)	1.2 (20)	1.2 (33)	0.5 (43)	0.5 (31)	0.4 (69)	0.4 (46)	0.9° (260)
I			0.3 (41)	0.4 (5)	0.3 (38)	0.3 (95)	0.3 (119)	0.3° (298)
Z			730	940	790	705	690	$770\,nT$

and (1b) is

$$C(\phi,\lambda,t) = n_{00}+n_{01}t+n_{02}t^2+n_{03}t^3+n_{04}t^4 + (\phi-\phi_c)(n_{10}+n_{11}t+n_{12}t^2) + (\lambda-\lambda_c)(n_{20}+n_{21}t+n_{22}t^2) \quad (2)$$

where t is the year of observations minus 1850, $\phi_c = 63°\,N$ and $\lambda_c = 26°\,E$. The coefficients n_{ij} were calculated using the method of least squares. The values used in the fits were those shown in Fig. 1 but also later values from secular points and from geomagnetic observatories were used in order to get the polynomials to fit to the present field as well as possible. Table 1 gives the coefficients n_{ij} and their standard deviations σ_{ij}. The numbers of observations used are shown in Table 2 (in brackets). The main figures in Table 2 are the r.m.s. differences between the observed and polynomial values grouped into 25-year period. The r.m.s. errors of Z were calculated from the r.m.s. errors of H and I.

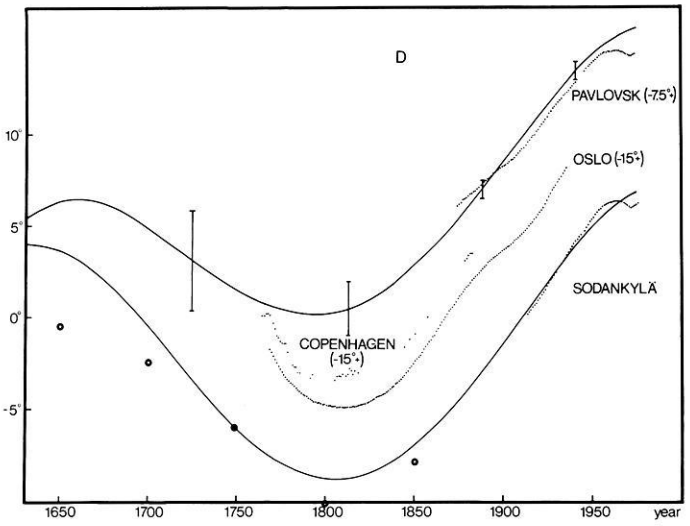

Fig. 2. Declination polynomials *(solid lines)* calculated for the magnetic observatories at Sodankylä and Pavlovsk (after 1947 Leningrad). *Dotted lines:* yearly means of observed values. *Circles: D* values taken from Barraclough's (1974) charts. *Vertical lines:* average r.m.s. error

Figures 2–4 show both polynomial and observed values of the H, D, and Z components for Sodankylä (67°22.2′N, 26°37,8′E) and Pavlovsk (59°41.2′N, 30°29.3′E) (after 1947 Leningrad) in the Soviet Union near the south-east border of Finland. To compare the polynomial values with observed ones not used in the least squares fits, yearly mean values from the geomagnetic observatory in Oslo (59°54.7′N, 10°43.4′E) compiled by Wasserfall (1950), D values from Copenhagen (55.69°N, 12.58°E) compiled by Abrahamsen (1973), and chart values of D from Barraclough (1974) have been included in Figs. 2–4.

As can be seen from Figs. 2–4, the polynomials give roughly the same shape as revealed by the long series of observatory values. Short-term variations can be seen in H and Z between 1890 and 1920 and in D after 1960. These variations are not visible in the polynomials because fourth degree time polynomials are too rigid to follow such rapid changes. The polynomials represent only the long-term (100 years or more) secular variation.

Systematic differencies between polynomial and observed values in Sodankylä are due partly to the sparse distribution of magnetic measurements in North Finland, but mainly to the fact that the Sodankylä observatory lies in a local Z anomaly covering at least 100×100 km. In 1975 the difference in Z between the chart value (Sucksdorff et al., 1975) and the annual mean value at Sodankylä was $600\,nT$ which is 10 times higher than the r.m.s. error for the whole Finland.

The D polynomials are more accurate than other components. They also extend about 150 years farther into the past than H and I. Even the extrapolated D for Sodankylä seems to fit the D values taken from spherical harmonic analysis for 1650–1850 (Barraclough, 1974).

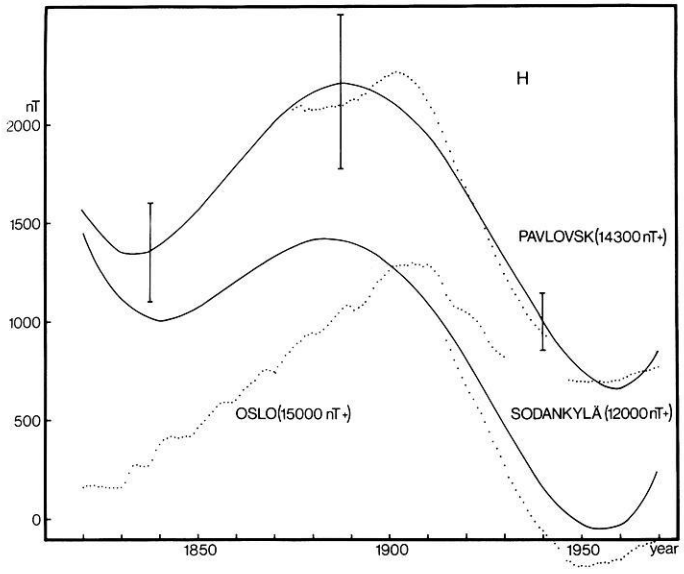

Fig. 3. Polynomials of the horizontal field *(solid lines)* calculated for the magnetic observatories at Sodankylä and Pavlovsk (after 1947 Leningrad). *Dotted lines:* yearly means of observed values. *Vertical lines:* average r.m.s. error

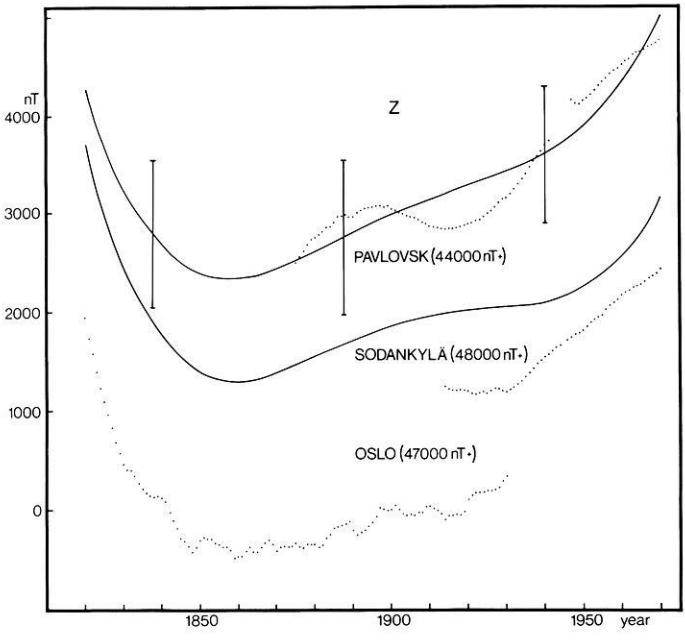

Fig. 4. Vertical field *(solid lines)* calculated from H and I polynomials for the magnetic observatories at Sodankylä and Pavlovsk (after 1947 Leningrad). *Dotted lines:* yearly means of observed values. *Vertical lines:* average r.m.s. error

Figure 2 also indicates that D changed cyclically with a period of about 400 years and an amplitude of 10°. It peaked around 1650 and dropped to a minimum around 1800, in agreement with other European records (Yukutake, 1962; 1967). The rapid oscillations since 1960 may forecast a new peak in the near future.

An interesting feature of the secular variation of Z (Fig. 4) is the rapid drop (c. $150\,nT$/year) at the beginning of the 19th century. From about 1850 to 1920 Z only increased slowly (c. $10\,nT$/year), but the secular change of Z has been faster in recent decades: 30–$50\,nT$/year.

The rate of westward drift of the geomagnetic field in Finland has been calculated from the polynomial values of D because its isolines flow roughly north to south, thus causing a maximum gradient in the east-west direction. The average drift for 1750 to 1950 was found to be 0.03 ± 0.01°/year averaged over Finland. This is rather a low value compared to the global average of 0.18°/year for the drift of the whole nondipole field found by Bullard et al. (1950), but roughly the same as that calculated by Leaton (1962) for the Finnish latitudes at the epoch 1955.0. On the other hand, Yukutake (1967) obtained an average drift of 0.36°/year when he studied the drift of D using observatory values all around the world in the last 300 years.

2. Sources of the Magnetic Field and Its Secular Variation in Finland and Nearby Countries

2.1. Equivalent Dipole

The global distribution of the geomagnetic field is usually analyzed by means of spherical harmonic expansions (SHA). Second and subsequent terms of these expansions give the contribution of the nondipole or anomaly field, which averages 20% of the whole field. The nondipole field is concentrated mainly in large centres of continental size, such as the one in Central Asia.

It is well known that changes of intensity and the westward drift of the nondipole field are the main sources of global secular variation (e.g., Yukutake and Tachinaka, 1968). The centres of the secular variation will be located near the centres of the anomaly field if the anomalies are standing and changing their intensity. If the anomalies are drifting, the secular variation centres will be located near the border of the anomaly centres. Nagata and Rikitake (1957) found that in most cases the focus of a secular variation cell lies west of the corresponding anomaly-field focus.

The surface anomaly field can be approximated by radial dipoles within the core (Alldredge and Hurwitz, 1964). The secular variation can be depicted by intensity changes and by the drift of these dipoles (Alldredge and Stearns, 1969), or directly by radial dipoles (Lowes and Runcorn, 1951).

The parameters, location (r_0, ϕ_0, λ_0) and strength (M), of these dipoles are usually determined from observed field values by the method of least squares. The dipole field equations are linearized and the parameters are then determined iteratively. To obtain converging solutions for the parameters, the

minimizing procedure must be started close enough to the minimum. This means that we need to know where the foci of the Z isolines are located and take these as initial values in the least-square fits.

Here, the features of the anomaly field will be interpreted based on one geocentric dipole. From the observed values of Z, H, and D at (ϕ, λ) it is possible to calculate the direction (ϕ_0, λ_0) and strength (M) of this dipole, here termed the equivalent dipole, which gives exactly the observed field at the observation points (ϕ, λ).

The equation of an equivalent dipole governing the total field vector, $\mathbf{B}=\mathbf{H}+\mathbf{Z}$, on the surface of the Earth at the point $\mathbf{R}=(R, \phi, \lambda)$, is

$$\mathbf{B}(\mathbf{R})=3(\mathbf{M}\cdot\mathbf{R})\mathbf{R}R^{-2}-\mathbf{M} \tag{3a}$$

where $\mathbf{M}$ is the strength of the dipole in Teslas (T) defined by

$$\mathbf{M}=(\mu_0/4\pi)\,\mathbf{M}_0 R^{-3} \tag{3b}$$

where $\mu_0/4\pi=10^{-7}\,Tm/A$ and M_0 is the dipole moment in units of $A\,m^2$.

The direction (ϕ_0, λ_0) of the equivalent geocentric dipole defining the 'north pole' or virtual geomagnetic pole (VGP), can be calculated from Eq. (3a) as follows:

$$\begin{aligned}
&\sin\phi_0=\sin\phi\cos\rho+\cos\phi\sin\rho\cos D\\
&\lambda_0=\lambda-A+180^\circ \quad \text{if } \cos\rho\geqq\sin\phi\sin\phi_0\\
&\lambda_0=\lambda+A \quad \text{if } \cos\rho<\sin\phi\sin\phi_0
\end{aligned} \tag{4a}$$

where

$$\begin{aligned}
&\sin A=\sin\rho\sin D/\cos\phi_0\\
&\tan\rho=2H/Z.
\end{aligned} \tag{4b}$$

See also McElhinny (1973). The strength $\mathbf{M}$ obtained from Eq. (3a), $\mathbf{H}$ and $\mathbf{Z}$, is

$$\mathbf{M}=\mathbf{H}-\mathbf{Z}/2 \tag{4c}$$

$$M=(H^2+Z^2/4)^{1/2} \tag{4d}$$

M defined by Eq. (4d) is also termed 'the local magnetic constant' after Bauer (1914), and it has been called 'the length of the dipole vector' by As (1967).

The global distribution of M and its secular variation has been analyzed by Gaibar-Puertas (1953) and As (1967). Ispir et al. (1976) have recently studied the secular variation of M over Turkey in 1965–1970.

If the observed field at every point (ϕ, λ) is a pure dipole field then M, ϕ_0 and λ_0 are constants:

$$\begin{aligned}
&M=(g_{10}^2+g_{11}^2+h_{11}^2)^{1/2}\\
&\tan\phi_0=g_{10}/(g_{11}^2+h_{11}^2)^{1/2}\\
&\tan\lambda_0=h_{11}/g_{11}
\end{aligned} \tag{5}$$

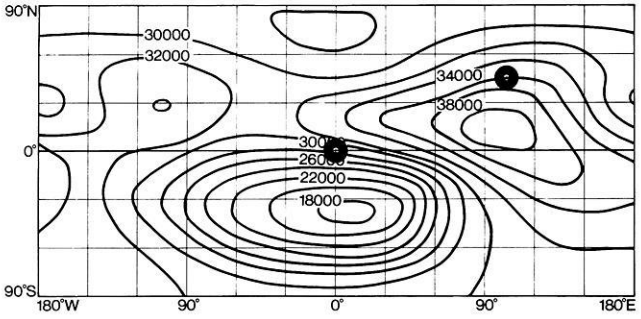

Fig. 5. Isolines (in nT) of the strength M of the equivalent dipoles calculated from IGRF-1965. The dots show Z foci of the Asian and African nondipole anomalies

where g and h are the gaussian coefficients of the spherical harmonic expansion of the magnetic field. Thus any deviation from these values is caused by the anomaly field. If, for example, the M values in a region are greater than the global average, this means there is a positive anomaly component in the observed magnetic field.

Although the isolines of M are related to those of the nondipole field, the foci of the M isolines do not coincide with those of the nondipole field. This can be seen in Fig. 5, which shows the global distribution of M calculated from the IGRF of 1965 (Zmuda, 1971). The M field consists of two large cells of isolines, one in Asia and the other covering Africa and the South Atlantic. The foci of these cells lie about 30° south of the corresponding nondipole centers in Central Asia and Africa.

Figures 6 and 7 show M and the location (ϕ_0, λ_0) of VGP's calculated from observed and polynomial values for Sodankylä, Pavlovsk and Oslo. Figure 6 gives locations of the geomagnetic pole calculated from the gaussian coefficients [Eq. (5)] obtained from SHA for 1840–1950 (Lucke, 1959). As can be seen, the curves for the equivalent dipole differ considerably from the values of the SHA field, which indicates the existence of a large nondipole field in Finland and nearby countries. The VGP's calculated from the Oslo values are nearest to the SHA geomagnetic pole, which means that the nondipole field in Scandinavia weakens from east to west. It can also be seen that the deviation from the SHA field has been growing steadily since the start of the 19th century. It can therefore be concluded that the nondipole field in Finland and nearby countries has been growing ever since. This is also true on a global scale as demonstrated by McDonald and Gunst (1967).

As can be seen in Fig. 6, the VGP's have been drifting westwards at an almost constant rate of 0.8°/year. This drift, however, is not necessarily connected with the general westward drift of the nondipole field, which was found to be 0.03°/year in Finland, as stated in Chap. 1. The rapid drift of the VGP's can also be explained by systematic intensity changes of the dipole and nondipole fields. By differentiating Eq. (4a), it can be shown that $d\lambda_0$ depends mostly on dD. In other words, the rapid westward drift of the VGP's is due to the linear growth of D (or Y) shown in Fig. 2.

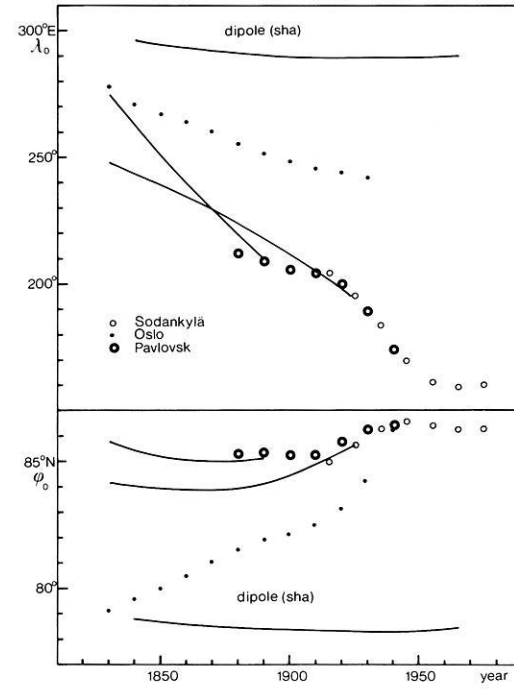

Fig. 6. Locations of the VGP's calculated from polynomials *(solid lines)*. The dots show 10-year means of VGP's calculated from observatory data. Also shown are the locations of the *sha* geomagnetic pole

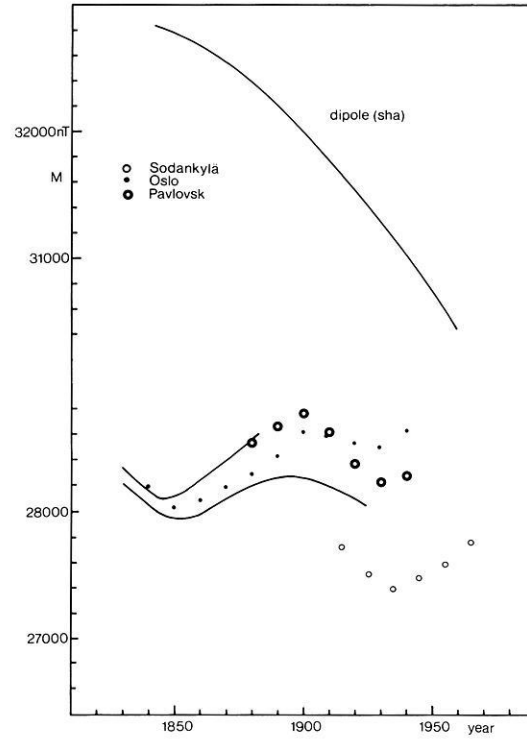

Fig. 7. Strength (M) of equivalent dipoles calculated from polynomials *(solid lines)*. The dots show 10-year means of M calculated from observatory data. Also shown is the strength of the *sha* dipole

Only 10% of the observed increase of D can be explained by changes of the SHA dipole and observed westward drift. Nearly all of the rapid increase of D has therefore been caused by the intensification of the Y component of the nondipole field.

As can be seen in Fig. 7, the curve calculated from the polynomials for the coordinates of Sodankylä differs about $500\,nT$ from the observations. This gap is due to the Z-anomaly covering the Sodankylä observatory.

2.2. *Eccentric Equivalent Dipole of the Secular Variation*

When radial dipoles are used to depict the secular variation, the dipoles must be located in the core near the core-mantle boundary, as shown by Lowes and Runcorn (1951) among others. For a more physical representation of the secular variation vector therefore, an eccentric equivalent dipole must be used instead of a geocentric one. Here we shall present a method for calculating an eccentric equivalent dipole of the secular variation vector starting from the geocentric equivalent dipole.

Using the secular variation vector, $\dot{\mathbf{B}}=\dot{\mathbf{X}}+\dot{\mathbf{Y}}+\dot{\mathbf{Z}}$, ($\dot{\mathbf{X}}=\Delta\mathbf{X}/\Delta t$, etc.), at (ϕ,λ), the magnitude $\dot{M}$ and the direction (ϕ_0,λ_0) of an equivalent geocentric dipole can be calculated from Eq. (4) if H, D, and Z needed in Eq. (4) are replaced by h, d, and z respectively defined by

$$h=(\dot{X}^2+\dot{Y}^2)^{1/2}$$
$$d=\tan^{-1}(\dot{Y}/\dot{X})$$
$$z=\dot{Z}. \tag{6}$$

The 'north pole' (ϕ_0,λ_0) of this dipole can be interpreted to be the virtual pole (focus) of the positive $\dot{Z}$ field.

Since the dipoles used here are radial, all the equivalent dipoles of a secular variation vector are located in the same diametral plane of the Earth. The intersection of this plane with the Earth's surface is a great circle, i.e., an S line, passing through the observations point and the poles of the equivalent dipoles. The orientation of this circle at a point (ϕ', λ') is defined by the declination D of the magnetic field of any equivalent dipole:

$$\cot D=\frac{\sin\phi'\cos\phi_0\cos(\lambda'-\lambda_0)-\cos\phi'\sin\phi_0}{\cos\phi_0\sin(\lambda'-\lambda_0)} \tag{7}$$

where (ϕ_0,λ_0) is the 'north pole' of the geocentric equivalent dipole of $\dot{\mathbf{B}}$. The total length (α) between the observation point and the pole (ϕ_0,λ_0) along an S line, is defined by

$$\cos\alpha=\sin\phi\sin\phi_0+\cos\phi\cos\phi_0\cos(\lambda-\lambda_0). \tag{8}$$

The distance (α') between the observation point and the north pole (ϕ'_0,λ'_0) of an eccentric dipole at q_0R from the geocentre ($q_0=0$ to 1) can be calculated from

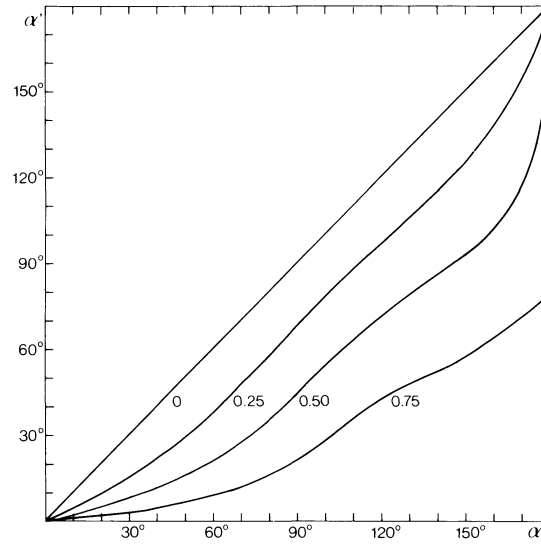

Fig. 8. Distance α' along an S line from the observation point to the pole (ϕ'_0, λ'_0) of an eccentric dipole at $q_0 = 0.0$, 0.25, 0.50, and 0.75, as a function of the distance α to the pole (ϕ_0, λ_0) of a geocentric equivalent dipole

the condition $I_e = I_c$ where I_e is the inclination of the eccentric and I_c that of a geocentric dipole at the point of observation. The equations for I_e and I_c are:

$$\tan I_e = \frac{f_z(\alpha', q_0)}{f_h(\alpha', q_0)} = \frac{\cos\alpha' - 3(\cos\alpha' - q_0)(1 - q_0\cos\alpha')\, r^{-2}}{\sin\alpha'(1 + 3q_0(\cos\alpha' - q_0)\, r^{-2})}$$

$$\tan I_c = \frac{f_z(\alpha, 0)}{f_h(\alpha, 0)} = \frac{-2\cos\alpha}{\sin\alpha}$$

$$r = (1 + q_0^2 - 2q_0\cos\alpha')^{1/2} \tag{9}$$

Figure 8 shows α' versus α when the eccentric dipole is at $q_0 = 0.0$, 0.25, 0.50, and 0.75. It can be seen that α is always greater than α', which means that the 'north pole' of a geocentric dipole, as seen by the observer, is always on the far side of the corresponding eccentric dipole. This far-side effect is similar to that noted by Wilson (1971), who found that paleomagnetic poles in the Tertiary and Quaternary ages tended to lie on the far side of the geographic pole, as seen from the region where the samples were taken. But calculating from an eccentric axial dipole, he obtained poles that were nearer the sampling sites and the geographic pole.

Figure 9 depicts $\dot{Z}_f/\dot{Z}'_f$, the ratio of $\dot{Z}$ at (ϕ_0, λ_0) to $\dot{Z}$ at (ϕ'_0, λ'_0), as a function of α

$$\dot{Z}_f/\dot{Z}'_f = f_z(\alpha', q_0) f_z(\alpha, 0)^{-1} (1 - q_0)^3 r^{-3}. \tag{10}$$

The corresponding ratios of dipole strengths $\dot{M}/\dot{M}'$ defined by Eq. (4d), can be obtained by multiplying the right hand term of Eq. (10) by $(1 - q_0)^{-3}$. From Fig. 9 it can be seen that $\dot{Z}_f/\dot{Z}'_f$ is about 1 and does not depend on q_0 when $\alpha < 60°$, but decreases rapidly when $\alpha > 60°$.

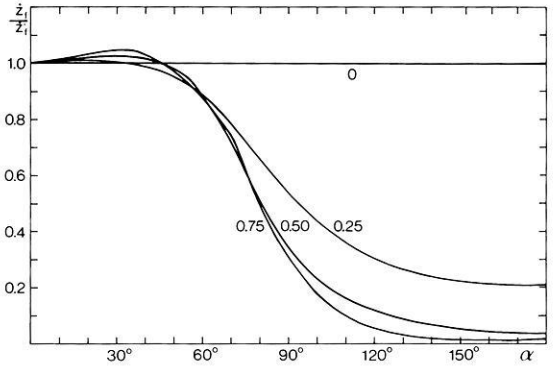

Fig. 9. $\dot{Z}_f/\dot{Z}'_f$ as a function of α, when eccentric equivalent dipole is at $q_0 = 0.0$, 0.25, 0.50, and 0.75. $\dot{Z}_f$ is $\dot{Z}$ at (ϕ_0, λ_0) and $\dot{Z}'_f$ is $\dot{Z}$ at (ϕ'_0, λ'_0)

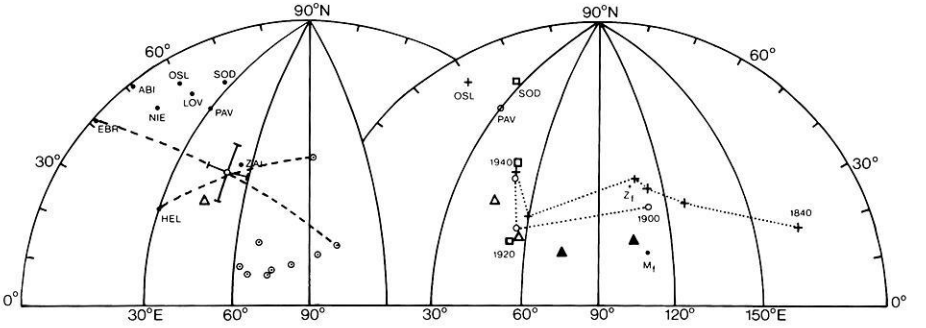

Fig. 10. *Left:* Poles (⊙) of geocentric equivalent dipoles of 10-year mean secular variation observed at nine observatories at 1940. ○ is the mean of the poles (ϕ'_0, λ'_0) of eccentric dipoles at $0.475R$ giving the minimum scatter of poles. Short *solid lines* show the area of 95% confidence around the pole. As examples, *S* lines are given for observatories Helwan *(HEL)* and Ebro *(EBR)*. △ is the focus of $\dot{Z}$ according to *SHA* maps of Cain and Hendricks (1967). *Right:* Path of the poles of eccentric ($q_0 = 0.475$) equivalent dipoles calculated from the secular variation observed at Sodankylä *(SOD)*, Oslo *(OSL)* and Pavlovsk *(PAV)* at 20-year intervals since 1840. △ is focus of $\dot{Z}$ of SHA maps for the epochs 1920 and 1940 by Cain and Hendricks (1967). ▲ is focus of isolines of M according to Gaibar-Puertas (1953) maps for the epochs 1900 and 1920. M_f is focus of the isolines of M from Fig. 5. Z_f is focus of *SHA* nondipole Z from IGRF-1965

The procedure for finding the parameters $(\phi'_0, \lambda'_0, \dot{M}')$ of the eccentric equivalent dipole of a secular variation vector $\dot{\mathbf{B}}$ observed at (ϕ, λ) is as follows:

– Calculate the geocentric equivalent dipole $(\phi_0, \lambda_0, \dot{M})$ and the length (α) of the *S* line using Eqs. (4), (6), and (8).
– Calculate α' for a given value of q_0 from Eq. (9).
– Calculate (ϕ'_0, λ'_0) from α' using Eqs. (7) and (8).
– Calculate $\dot{M}'$ using Eq. (10).

If several observations covering a large area are available, a best fitting dipole can be determined by minimizing the scatter of the poles (ϕ'_0, λ'_0) found for each vector $\dot{\mathbf{B}}$. An example of this is given in Fig. 10, which shows the poles of the geocentric and the best fitting dipoles of the secular variation at nine

Table 3. Fisherian statistics for a best fitting eccentric dipole of the secular variation at the epoch 1940

$\phi_0 = 46.2° N$	$N = 9$
$\lambda_0 = 50.6° E$	$\alpha_{95} = 9.8°$
$q_0 = 0.475$	$k = 205$

European observatories at the epoch 1940. The minimum scatter was found by changing q_0 and calculating Fisher's precision parameter k (Fisher, 1953) for the corresponding values of (ϕ'_0, λ'_0). The scatter is at its minimum when k is at its maximum. The best fitting dipole was found to lie at $46.2° N$, $50.6° E$, and $0.475\,R$ from the centre of the Earth. Its strength was $-8.1\,nT$/year; see also Table 3 and Fig. 10. This best fitting dipole gives $\dot{Z}$, $\dot{X}$, and $\dot{Y}$ at the observatories used with r.m.s. errors of $6.4\,nT$/year, $7.3\,nT$/year and $4.0\,nT$/year respectively.

The location of the mean pole found here is fairly close to the focus ($36° N$, $45° E$) of $\dot{Z}$ on the SHA map Cain and Hendricks (1967), which lies almost within the area of 95% confidence for the mean pole. The distance q_0 in Table 3 is near the core-mantle boundary, same as that found by Lowes and Runcorn (1951) for their dipoles.

The relatively small area of scatter of the poles in the left-hand side of Fig. 10 indicates that secular variation in Europe and West Asia has a common source. The right-hand side of Fig. 10 shows the probable movements of the pole of this source since 1840. It is based on eccentric equivalent dipoles ($q_0 = 0.475$) of the secular variation observed at Sodankylä, Oslo and Pavlovsk. The poles appear to have been drifting westwards at a rate of 1°/year. The path of the poles lies in the area of high intensity of the SHA nondipole field, indicating a correlation between the secular variation in North Europe and the anomaly field in Asia. This correlation seems to prevail over a large area of Eurasia, because the focus of the isolines of $\dot{M}$ taken from Gaibar-Puertas (1953) global chart has been moving along a path near the focus of the Asian anomaly, as can be seen in the right-hand side of Fig. 10.

Figure 11 depicts the intensity $\dot{M}$ of the geocentric equivalent dipoles. Striking features in the variations of $\dot{M}$ are the sharp minimum just before 1900, the rapid, almost threefold increase in the subsequent 20 years, and other rapid drop to a minimum around 1960. Observed focal values of $\dot{Z}$ taken from SHA maps (Cain and Hendricks, 1967), reduced to the centre of the Earth show roughly the same decreasing trend as those calculated from the observatory values.

$\dot{M}$ in Fig. 11 oscillates in a cycle of approximately 60 years, which is in phase with the curves of the variation of the Earth's rotation found by Yukutake (1972; 1973) and Jin and Thomas (1977). According to these authors, the variation in the length of the day correlates well with the general 60-year oscillation of the Earth's magnetic field. So, it is suggested here that the variation of the equivalent poles and their intensities, and the change of the SHA $\dot{Z}$ focus in South-west Asia are caused by the 60-year oscillation of the magnetic field in the Asian nondipole anomaly.

The focus of the 60-year oscillation of the secular variation in Europe has also been determined, using other methods, by Barta (1978) and Golovkov and

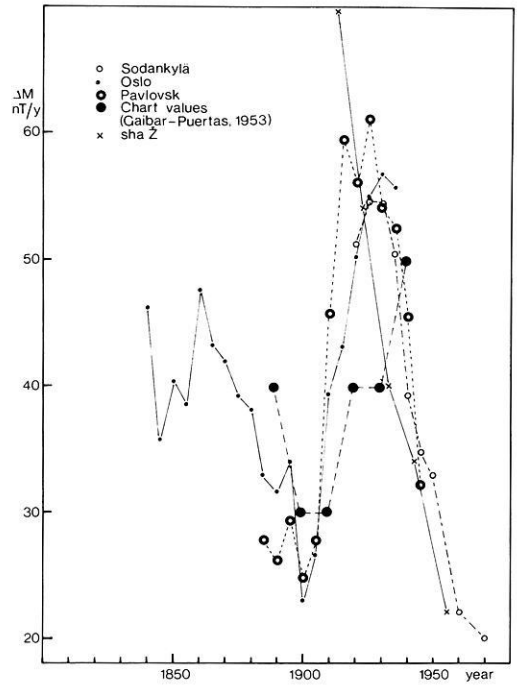

Fig. 11. Ten-year means of the intensity $\dot{M}$ of the geocentric equivalent dipoles calculated from secular variation data

Kolomiytseva (1971), who found foci at (28° N, 68° E) and (27° N, 41° E) respectively. These foci are near the path of the equivalent poles shown in Fig. 10.

Conclusions

The polynomials calculated for the magnetic field in Finland before 1970 reveal only the general trend of the magnetic field and its secular variation. They fail to disclose periods of rapid variations registrated at magnetic observatories between 1890 and 1920.

As could be expected, accuracy was best in the D polynomial, which revealed the declination in Finland with a maximum error of 3° from 1650 to 1850, and less than 1° after 1850.

The rather low value of the westward drift found here means that the drift, though global, is not an important source of secular variation in Finland. The intensification of the SHA nondipole field, especially its Y component, seems to be the major source of secular variation in Finland and nearby countries during the last 150 years.

The equivalent dipole method applied here can be used to locate source regions of secular variation. It was found that a single source has been dominated the secular variation in Europe during the past 150 years.

Because the SHA dipole part of the observed field **B** is usually much stronger than SHA nondipole part, the equivalent dipole method cannot be used

to locate SHA nondipole centers. But if the geocentric equivalent dipole is calculated for large areas at a given epoch, any variation of intensity and direction of the dipole can be assumed to be caused by the SHA nondipole field because the contribution of the SHA dipole field to the equivalent dipole parameters is constant. The method thus reveals the existence of an SHA nondipole anomaly at the point of observation.

Acknowledgement. This study was financially supported by Suomen Tiedeseuran Sohlbergin delegaatio.

References

Abrahamsen, N.: Magnetic secular variation in Denmark, 1500–1970. J. Geomagn. Geoelectr. **25**, 105–111, 1973

Alldredge, L.R., Hurwitz, L.: Radial dipoles as the sources of the Earth's magnetic field. J. Geophys. Res. **69**, 2631–2640, 1964

Alldredge, L.R., Stearns, C.O.: Dipole model of the sources of Earth's magnetic field and secular variation. J. Geophys. Res. **74**, 6583–6593, 1969

As, J.: Past, present and future changes in the Earth's magnetic field. In: Magnetism and Cosmos, W.R. Hindmarsh, F.J. Lowes, P.H. Roberts, S.K. Runcorn, eds.: pp. 29–44. Edinburgh: Oliver and Boyd Ltd. 1967

Barraclough, D.R.: Spherical harmonic analyses of the geomagnetic field for eight epochs between 1600 and 1910. Geophys. J. R. Astron. Soc. **36**, 497–513, 1974

Barta, G.: Secular variation of the terrestrial magnetic field and the internal structure of the Earth. In: Electromagnetic field of the Earth, M. Hvozdara, ed.: pp. 49–58. Bratislava: Publishing House of the Slovak Academy of Sciences 1978

Bauer, L.A.: The local magnetic constant and its variation. Terr. Mag. Atmos. Electr. **19**, 113–125, 1914

Bullard, E.C., Freedman, C., Gellman, H., Nixon, J.: The westward drift of the Earth's magnetic field. Philos. Trans. Soc. London, Ser. A **234**, 67–92, 1950

Cain, C.C., Hendricks, S.: The geomagnetic secular variation, 1900–1965, Greenbelt, Md.: Goddard Space Flight Center September 1967.

Fisher, R.A.: Dispersion on a sphere. Proc. Soc. London Ser. A: **217**, 295–305, 1953

Gaibar-Puertas, C.: Variación secular del campo geomagnético. Observatorio del Ebro Memoria, No. **11**, 1953

Golovkov, V.P., Kolomiytseva, G.I.: Morphology of 60-year geomagnetic field variations in Europe. Geomagn. Aeron. **11**, 571–574, 1971

Ispir, Y., Isikara, A.M., Özden, H.: Variation in the local magnetic constant and seismicity of Turkey. J. Geomagn. Geoelectr. **28**, 137–143, 1976

Jin, R., Thomas, D.M.: Spectral line similarity in the geomagnetic dipole field variations and length of day fluctuations. J. Geophys. Res. **82**, 828–834, 1977

Leaton, B.R.: Geomagnetic secular variation for the epoch 1955. O. R. Obs. Bull. **57**, 245–270, 1962

Lowes, F.J., Runcorn, S.K.: The analysis of the geomagnetic secular variation. Philos. Trans. R. Soc. London, Ser. A: **243**, 525–546, 1951

Lucke, O.: Analyse der Veränderungen des Erdmagnetischen Hauptfeldes, aus den Potentialentwicklungen erschlossen. In: Geomagnetismus und Aeronomie, Band III, G. Fanselau, ed.: pp. 217–312. Berlin: Deutscher Verlag der Wissenschaften 1959

McDonald, K.L., Gunst, R.H.: An analysis of the Earth's magnetic field from 1835 to 1965. ESSA Tech. Rep., IER 46-IES 1, 1967

McElhinny, M.W.: Paleomagnetism and plate tectonics. Cambridge: Univ. Press 1973

Nagata, T., Rikitake, T.: Geomagnetic secular variation during the period 1950–1955. J. Geomagn. Geoelectr. **9**, 42–50, 1957

Nevanlinna, H., Sucksdorff, C.: Magnetic field in Finland, 1800–1970. Finn. Met. Inst. Stud. Earth Magn. **25**, 1976

Sucksdorff, C., Nevanlinna, H., Welling, P.: Magnetic charts of Finland for 1975. 0. Finn. Met. Inst. Stud. Earth Magn. **24**, 1975

Wasserfall, K.F.: A study on the secular variation of magnetic elements based on data for *D*, *I*, and *H* for Oslo, 1820–1938. J. Geophys. Res. **55**, 275–300, 1950

Wilson, R.L.: Dipole offset – The time average paleomagnetic field over the past 25 m. y. Geophys. J. R. Astron. Soc. **22**, 491–504, 1971

Yukutake, T.: The westward drift of the magnetic field of the Earth. Bull. Earthq. Inst. **39**, 427–476, 1962

Yukutake, T.: The westward drift of the Earth's magnetic field in historic times. J. Geomagn. Geoelectr. **7**, 1–14, 1967

Yukutake, T.: The effect of change in the geomagnetic dipole moment on the rate of the Earth's rotation. J. Geomagn. Geoelectr. **24**, 19–47, 1972

Yukutake, T.: Fluctuations in the Earth's rate of rotation related to changes in the geomagnetic dipole field. J. Geomagn. Geoelectr. **25**, 195–212, 1973

Yukutake, T., Tachinaka, H.: The westward drift of the geomagnetic secular variation. Bull. Earthq. Inst. **46**, 1075–1102, 1968

Zmuda, A.J.: World Magnetic Survey. IAGA Bull. **28**, 1971

Received March 22, 1979; Revised Version July 11, 1979; Accepted August 10, 1979

J. Geophys. 46, 217–224, 1979

Journal of Geophysics

Age and Crustal Structure of the Canary Islands

A Discussion

H.-U. Schmincke

Institut für Mineralogie, Ruhr-Universität, Universitätsstr. 150,
D-4630 Bochum, Federal Republic of Germany

Abstract. The postulation of a Mesozoic age for the shield-building basaltic series of Gran Canaria and Tenerife by Storevedt et al. (1978), based upon paleomagnetic data from these islands, is inconsistent with abundant and concordant K/Ar-ages from several laboratories. These latter data leave no doubt that no rocks older than Mid-Miocene have been found on Gran Canaria and Tenerife. Moreover, no volcaniclastic layers older than Miocene were found in Deep Sea Drilling cores near the Canary Islands. Also, the volcanic apron around at least Gran Canaria appears to be Miocene in age judging from seismic reflectors that extend to well-dated drilled sections. There is no evidence for a sialic crustal layer extending beneath all or any of the Canary Islands.

Key words: Canary Islands – Crustal structure – Volcanic Islands – Potassium Argon Ages – Paleomagnetism.

1. Introduction

Storetvedt et al. (1978) have used paleomagnetic data from Gran Canaria and Tenerife to postulate that the Canary Islands were built up during two major volcanic pulses, the first occurring in the Mesozoic (Late Cretaceous or earlier) and the second during Late Tertiary. They also propose that their data, combined with other lines of evidence, favor 'a continental origin of a crustal belt (including the Canary Islands) extending seaward into water depths of at least 4,500 m'.

Storetvedt et al. (1978) appear to have overinterpreted their data and those from the literature, and several relevant papers were not discussed:

A variety of geophysical and geological studies (see below) have been carried out in this part of the Atlantic (off the northwest coast of Africa) during the last fifteen years, this being a key target area in studying the evolution of passive continental margins. The conclusions of Storetvedt et al. (1978) will, therefore, be discussed in detail, using published and some unpublished material.

0340-062X/79/0046/0217/$01.60